Modeling of the kinetics of sulphation of CaO particles under CaL reactor conditions

*J.M. Cordero, M. Alonso**

Instituto Nacional del Carbón, CSIC, C/Francisco Pintado Fe, No. 26, 33011 Oviedo, Spain

*Phone: 34-985 119 090, Fax: 34-985 297 662, e-mail: mac@incar.csic.es

ABSTRACT

CO_2 capture in a calcium looping (CaL) system is one of the most promising technologies for climate change mitigation. The main reactors in these systems (carbonator and calciner) operate in conditions where the reaction of CaO with the SO_2 resulting from the combustion of coal is inevitable. This work reports on the sulphation of CaO under a range of variables that are typical of reactors in CaL systems. Furthermore it is demonstrated that the number of calcination carbonation cycles changes the sulphation patterns of the CaO from heterogeneous to homogeneous in all the limestones tested. For 50 carbonation calcination cycles and for particle sizes below 200 μm, the sulphation pattern is in all cases homogeneous. The sulphation rates were found to be first order with respect to SO_2, and zero with respect to CO_2. Steam was observed to have a positive effect only in the diffusion through the product layer controlled regime, as it leads to an improvement in the sulfation rates and effectiveness of the sorbent. Most of the experimental results of sulfation of highly cycled sorbents under all conditions can be fitted by means of the Random Pore Model (RPM) assuming that the kinetics and diffusion through the product layer of the $CaSO_4$ are the controlling regimes.

Keywords: sulphation kinetics, SO_2 capture, calcium looping, CO_2 capture, RPM, CFB

1. Introduction

CO_2 capture and storage is one of the best options for mitigating CO_2 emissions to the atmosphere and climate change [1]. Among the technologies developed, the post-combustion calcium looping (CaL) system is one of the most promising due to the economic benefits it offers and experience acquired with similar systems already operating at industrial scale [2-7]). One of the main advantages of these emerging CaL technologies is the low cost of the sorbent since natural limestone is used as the preferred source of CaO. Figure 1 represents one of the possible configurations of a full post-combustion CaL system for capturing CO_2 consisting of three main reactors functioning as CFBs (including in this diagram the CFBC power plant as the source of flue gases). In this configuration, coal is burned in air in the CFBC, generating a stream of gases that is fed to the CFB carbonator, which operates at around 650 °C. It is here that CO_2 capture takes place since the CaO reacts with CO_2 to form $CaCO_3$. The carbonated solids then enter the CFB calciner, where CaO is regenerated to form a rich CO_2 atmosphere typical of oxy combustion at temperatures of around 900 °C [2]. The high temperatures at which both the CFB carbonator and CFB calciner operate allow efficient heat integration by generating different streams of solids and gases at high temperatures. The rapid development of this technology can be attributed to its similarity to existing CFBC power plants.

The viability of this technology has been demonstrated in several pilot plants including La Pereda (Spain) which produces 1.7 MWth and is the largest CaL for CO_2 capture installed so far [8, 9]. Other pilots that have achieved promising results are the 1 MWth pilot plant in Darmstadt (Germany) [10], the 0.3 MWth pilot in La Robla [11], the 0.2 MWth pilot at Stuttgart University (Germany) [12] and the 1.9 MWth pilot that is being

constructed in Taiwan [13], apart from smaller projects that have also reported positive results [14-16].

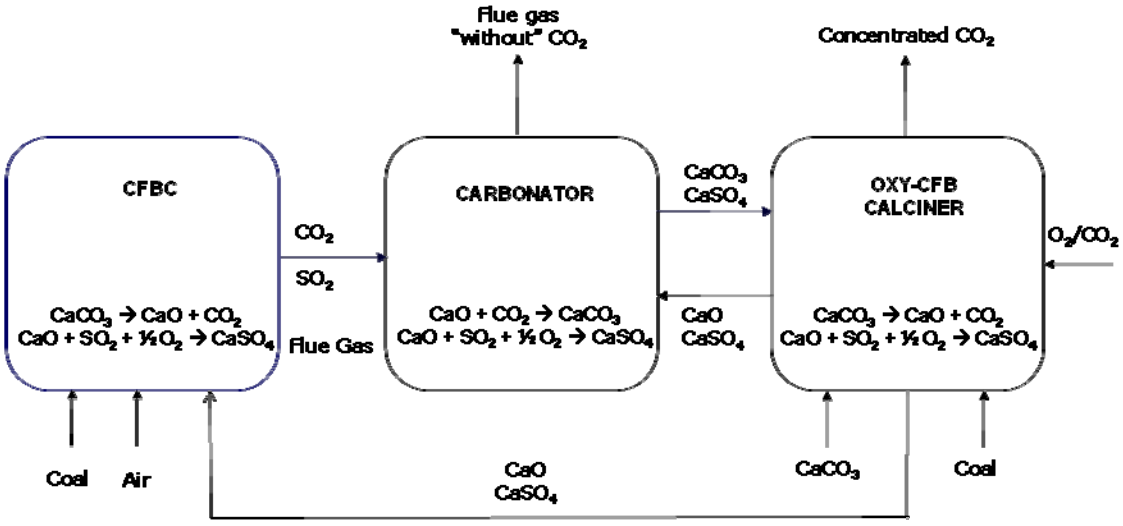

Figure 1. Principal reactors of a CaL system integrated with a CFBC and its main variables.

A synergy can be exploited in this scheme if the purge extracted from the CaL CO_2 capture system is injected into the CFBC to be used as a calcium sorbent in substitution for the fresh limestone that is routinely used for desulfurization [17-19]. A recent paper [20] illustrates with mass and energy balances the operational and fuel composition windows that make this synergy possible. SO_2 is produced in the CFBC as well as in the oxy CFB calciner due to the combustion of coal. It can also enter into the CFB carbonator depending on the power plant's SO_2 removal efficiency. Under the operating conditions of all three main CFB reactors, SO_2 will react with CaO to form $CaSO_4$ which will not decompose at these working temperatures due to its thermodynamic equilibrium. Furthermore, a certain quantity of $CaSO_4$ in the CaL system is guaranteed depending on the amount of fresh makeup limestone and purge. Therefore, SO_2 will deactivate the CaO available for CO_2 capture [21-23]. The deactivation would be

enhanced if methods of reactivation like recarbonation [24] or hydration [25] were used to reduce the make-up.

There is a large background of literature on the sulphation of CaO particles under combustion conditions [26-39]. However, there are several novel features in the CaL system of Figure 1 that have not yet been sufficiently dealt with in the literature. The main novelty is that the particles of a CaL undergo a certain number of calcination carbonation cycles that promote a sintering mechanism characterized by a widening of the pores and a reduction of the surface area [40]. This effect could lead to an enhancement of SO_2 capture as there is more effective space available for housing the $CaSO_4$ formed, leading to higher CaO conversions [26, 41]. Another difference is related to the operating temperatures of the system schematized in Figure 1. These can vary from 650 °C in the CFB carbonator to 930 °C in the oxy CFB calciner, whereas most sulphation studies are conducted at temperatures of around 850 ºC (the typical temperature in CFBC power plants). The reaction atmosphere also varies from one reactor to another: in CFBCs an average CO_2 concentration of 10% vol. is usual whereas a CO_2 concentration higher than 70 % vol. is to be expected in an oxy-fired CFB calciner. Finally, the conversions of CaO to $CaSO_4$ predicted by the mass balance applied to the CaL system will not exceed 0.1 due to the Ca/S ratio in these systems is larger than in a desulfuration system. This will avoid the extensive pore blockage typical of sulphation in FB combustors, where the aim is to ensure maximum sorbent conversion for sulphation to occur.

The sulphation of CaO has been extensively investigated and consequently particle sulfation models have been developed with the objective of integrating them into larger reactor models. These particle models can be basically divided into two types: grain and pore models. The original grain models assumed that particles are formed by smaller

blocks called grains (sometimes referred to as micro grains) [29, 42]. These grains are assumed to be of uniform size, spherically shaped and non-porous. The reaction follows the shrinking core model and no structural changes are taken into consideration. Later, the grain models evolved, taking into consideration other grain or micro-grain geometries such as cylindrical or flat [42, 43], structural changes in the grains [31, 44-47], and grain size distribution [43, 48].

The initial pore models assumed that the particles were traversed by pores that are usually cylindrically shaped. These pores were supposedly of uniform size and randomly intersected [49, 50]. This type of model developed taking into account the initial pore structure and its transformation as the reaction proceeds. The pore structure in this model was explained in terms of the evolution of the pore size distribution. Simons et al. [51] assumed that the distribution is like a complex tree where the pore size decreases the further inside the particle the pore is. One of the most widely used pore models is the model developed by Bhatia and Perlmutter [52, 53]: the random pore model (RPM), which assumes that the particle is traversed by random size cylindrical pores with intersecting and overlapping surfaces as reaction proceeds. This model was applied successfully to gas solid reactions [54] including the carbonation and sulphation of CaO [33, 54-57].

The present work focuses on the modelling of the sulphation rates and retention capacities of CaO in the three main reactors involved in CaL, taking into account the special features of these systems and the fact that the sorbent is composed of particles with a specific number of cycles.

2. Experimental

Three different limestones with particle sizes of 36-63 μm, 63-100 μm, 100-200 μm and 400-600 μm were used to study the sulphation reaction of the CaO particles under

different conditions. Their chemical composition was measured by optical induced coupled plasma mass spectrometry (optical ICP-MS) and it is shown in Table 1.

Table 1. Chemical composition (wt %) of the limestones used in this work

	Al_2O_3	CaO	Fe_2O_3	K_2O	MgO	Na_2O	SiO_2	TiO_2
Compostilla	0.16	89.7	2.5	0.46	0.76	<0.01	0.07	0.37
Enguera	0.18	98.9	<0.01	0.03	0.62	0.00	0.43	0.02
Brecal	0.00	98.4	0.10	0.00	0.78	0.00	0.69	0.00

Enguera and Brecal are high purity limestones whereas Compostilla is the limestone of lowest purity. The most prominent of impurities are Fe_2O_3, K_2O and TiO_2.

For the sulphation tests, the thermogravimetric analyzer system illustrated in Figure 2a was used. It consists of a microbalance from CI Instruments, which continuously measures the weight of the sample suspended on a flat platinum pan inside a quartz tube. A special characteristic of its design is the two-zone furnace that can be moved up and down by means of a pneumatic piston. This allows a rapid change between carbonating and calcining temperatures when performing calcination carbonation cycles. The movement of the piston can be synchronized with changes in the gas fed to the TGA by means of mass flow controllers. The temperature of the sample is measured with a thermocouple located very close to the platinum basket and is continuously recorded, as is the weight of the sample by a computer.

A preliminary study was conducted in order to avoid external diffusional effects. The superficial gas velocity was set at 0.06 m/s (650 °C) for both the sulphation and carbonation reactions since experiments performed at half of this superficial gas velocity had no effect on the rates measured. It is well known that the initial sample

mass influences the external diffusional effects. A sample mass of 2-3 mg was small enough to neutralise the diffusional effects as no appreciable changes were detected in the initial sulphation rate, as can be seen in Figure 2b.

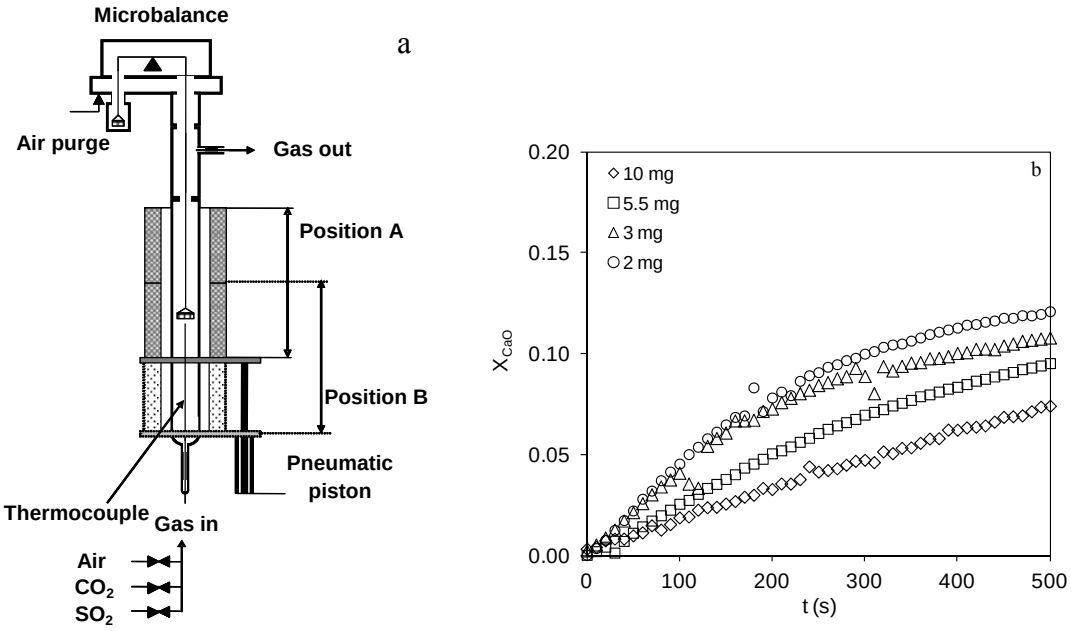

Figure 2. Schematic of the experimental setup used in this work (a). Effect of the initial sample mass on the experimental sulphation rate (b); particles of 63-100 μm, 500 ppmv SO_2 in air, 650 °C, with sulphation occurring after only one calcination (N = 1).

In the experimental procedure employed in this study before the sulphation tests the sample was subjected to the desired number of calcination carbonation cycles. The carbonation of the samples was carried out in an atmosphere of 10% vol. CO_2 in air, at 650 °C, and the calcination was conducted in air at 930 °C (a blank test confirmed that the use of pure CO_2 is unnecessary during calcination to obtain a specific texture linked to a certain cycle number). Each stage of calcination or carbonation was 10 minutes long as these conditions enable comparable sorbent morphologies to those expected in the system of Figure 1 [58]. Finally, after the temperature had stabilized, the sulphation stage was initiated. The conversion of CaO to $CaSO_4$ was calculated from the weight gain of the samples.

Table 2. Porous structural parameters for the limestones used in this work.

	S_0 (m^2/m^3) x 10^7	ε	L_0 (m/m^3) x 10^{14}	d_{pm} (nm)	ψ	X^*_{CaO}
Compostilla	4.58	0.40	4.79	33.0	1.7	0.32
Enguera	3.90	0.45	3.29	40.7	1.5	0.39
Brecal	4.37	0.42	4.12	35.6	1.6	0.35

In order to obtain the initial pore parameters of the materials shown in Table 2, a mercury porosimeter Autopore IV 9500 by Micromeritics was used. The samples were previously calcined in a furnace in air at 930 °C. All the sorbents were mesoporous, with the average pore size ranging from 33 to 40.7 nm. The measured porosities indicate that all the sorbents underwent shrinkage during calcination. It was this shrinkage that gave place to a maximum sulphation conversion in the interior of the particles of 0.32 to 0.39, as calculated from the mass balance equation (1) [33]:

$$X^*_{CaO} = \frac{\varepsilon_0}{(1-\varepsilon_0)(Z-1)} \quad (1)$$

Being Z the ratio between the volume of solid phase after reaction to that before reaction. It was estimated as V_{MCaSO4}/V_{MCaO}. Some samples were selected to examine the $CaSO_4$ distribution in the particles. For this purpose a Quanta FEG 650 scanning electron microscope (SEM) coupled to an energy dispersive X ray (EDX) analyser Ametek EDAX equipped with an Apollo X detector was used. The samples were embedded in a Recapoli 2196 resin, cross sectioned and polished.

3. Description of the reaction model

In order to determine the sulphation pattern of the CaO particles, a SEM-EDX analysis was conducted on selected samples. Back scattered electrons (BSE) were used because they show differences in chemical composition by displaying higher molecular weight compounds in brighter colours than lower molecular weight compounds. The BSE-SEM photographs (left side) are supported by EDX mapping to show the sulphur distribution (right side).

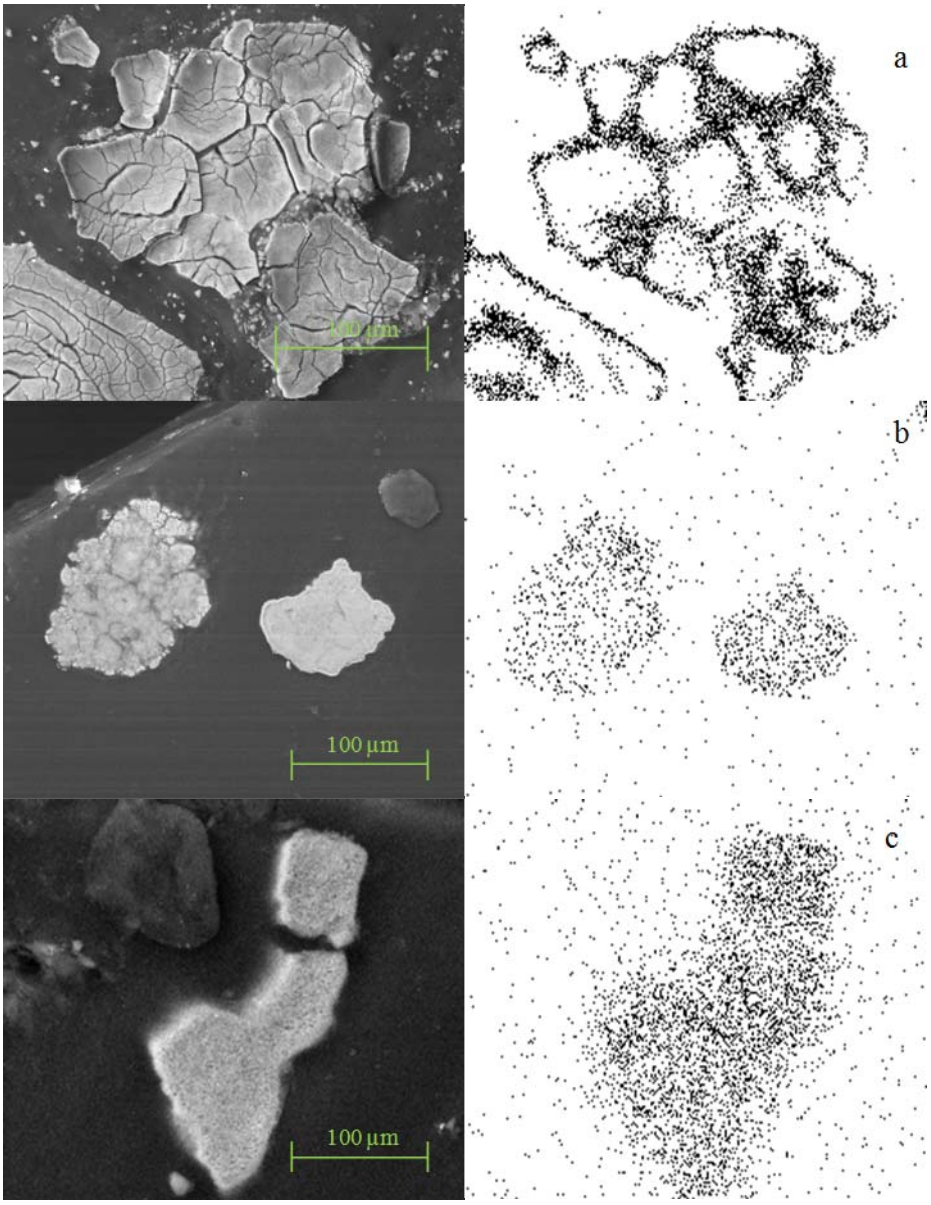

Figure 3. SEM EDX for (a) lime with a $CaSO_4$ conversion of 0.12 sulphated after one calcination, showing an unreacted core sulphation pattern (b) lime with a sulphation

conversion of 0.32 after 50 calcination-carbonation cycles and (c) lime with a conversion of 0.25 after 50 calcination-carbonation cycles showing homogeneous $CaSO_4$ distributions.

Figure 3a shows particles obtained from a calcined limestone sulphated under a CFB calciner conditions. BSE-SEM shows that the $CaSO_4$ is concentrated on the external surface (brightest colours), as is confirmed by EDX, the sulphur spots being more thinly scattered in the centre of the particles. The sulphation pattern follows the unreacted core pattern. However, for sulphated particles after 50 cycles (Figure 3b-c) there are no appreciable differences in colours in the BSE-SEM, and the EDX indicates a homogeneous distribution of the sulphur throughout the particles. These semi-quantitative results reveal that the sulphation pattern is of the unreacted core type when the number of cycles is low and close to 1 and homogeneous when the number of cycles is sufficiently high.

In order to provide a reasonable interpretation of the experimental results and scalable information on the kinetic parameters derived from the experiments conducted in this study, a discussion of the sulphation patterns and key model assumptions is presented. Several different sulphation patterns have been described in relation to the $CaSO_4$ distributions in the particles [41]. There are three basic sulphation patterns. The unreacted core pattern is characterized by external pore blockage of the surface due to differences in the molar volumes of the $CaSO_4$ and CaO (52.2 and 16.9 cm^3/mol respectively). This pore blockage hinders further sulphation of the inner core of the particles, thus inhibiting the conversion of CaO to $CaSO_4$. The unreacted core pattern is characteristic of sorbents with micro-pores that have no fractures, so only the external surface becomes sulphated, the inner part of the particles remaining unsulphated or only slightly sulphated. The network pattern is characteristic of particles of sorbent with an

interconnected network of micro-fractures that allows SO_2 to penetrate inside the particles and to form sulphate inside them in the proximity of the fractures. In this pattern, the particles are divided by the fractures into blocks, each block behaving like an unreacted core since only the external surface, corresponding to the fractures, achieves a high degree of sulphation. Finally, the homogeneous pattern is typical of small particles with wide pores and interconnected fractures. The SO_2 can reach all the surfaces, ensuring a uniform sulphation of the particles. All of these patterns were found in the sulphation of fresh calcined limestones depending on the initial structural properties of the calcined sorbent [26, 41, 59]. However, in a postcombustion CaL system, there are other factors that can change the expected sulphation pattern. One of these factors is the number of calcination-carbonation cycles since they modify the initial porous structure of the particles. Cycling of the sorbent produces sintering: a reduction of the surface area and an enlargement of the pore size [40]. Another factor is the temperature at which the reaction takes place since each reactor has a different temperature. High temperatures increase the diffusional resistance of the reactant in the pores, and as a consequence pore blockage is more likely to occur. Another limitation is the particle size, since the higher the particle size is, the more likely it is that a core sulphation pattern will occur. Therefore, unreacted core sulphation patterns are more likely for low numbers of calcination carbonation cycles and in the calciner, whereas pseudo or homogeneous sulphation patterns are more likely to occur with highly cycled particles and in the carbonator, as shown in Figure 4.

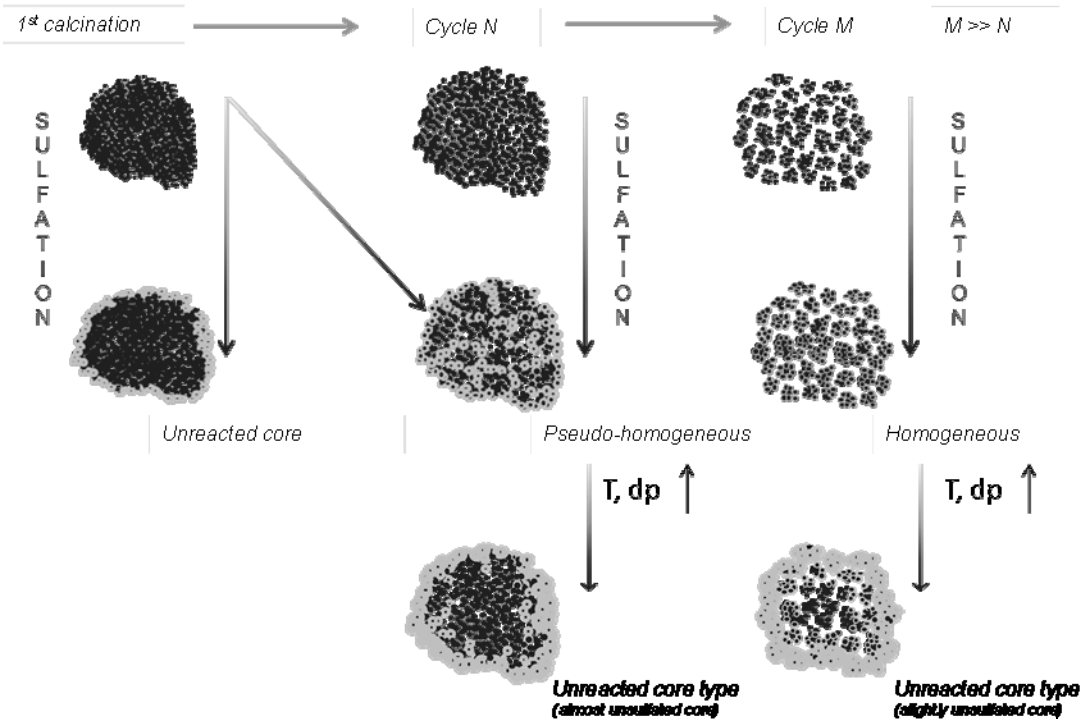

Figure 4. Schematic of the distribution of $CaSO_4$in the particles as a function of the number of calcination carbonation cycles (N), the temperature (T) and the particle diameter (dp).

From the above qualitative discussion of sulfation patterns it is clear that the Random Pore Model is a suitable model for fitting the kinetic parameters and for developing the mathematical expressions to predict the experimental conversion curves of CaO to $CaSO_4$ in the range of operation of the three main reactors involved in post combustion CaL systems. The main reactions to be considered are:

$CaCO_3 \rightarrow CaO + CO_2$ (1)

$CaO + SO_2 + 1/2O_2 \rightarrow CaSO_4$ (2)

$CaO + CO_2 \rightarrow CaCO_3$ (3)

where reactions (1) and (2) take place in the CFBC and in the oxy CFB calciner, while reactions (2) and (3) occur in the CFB carbonator, as shown in Figure 1.

Further assumptions for the RPM are that:

-The particles are isotherm.

-The diffusional effects in the pores are negligible (no radial concentration profiles).

-The sulphation reaction is first order with respect to the SO_2 concentration.

In these conditions, the expression of the RPM model that is valid for the kinetic control and diffusional control of the reactant SO_2 through the product layer of $CaSO_4$ is [53]:

$$\frac{dX_{CaO}}{dt} = \frac{k_s S C_s (1 - X_{CaO}) \sqrt{1 - \psi \ln(1 - X_{CaO})}}{(1 - \varepsilon)\left[1 + \frac{\beta Z}{\psi}\left(\sqrt{1 - \psi \ln(1 - X_{CaO})} - 1\right)\right]} \tag{2}$$

where ψ is the internal structure parameter that accounts for the internal structure of the particle and is expressed as:

$$\psi = \frac{4 \pi L (1 - \varepsilon)}{S^2} \tag{3}$$

and β is:

$$\beta = \frac{2 k_s a \rho (1 - \varepsilon)}{b M_{CaO} D_P S} \tag{4}$$

There are two extreme cases for equation (2) where the kinetic equation can be further simplified. Under the fast kinetic regime (i.e. $\beta = 0$) [52]:

$$\frac{dX_{CaO}}{dt} = \frac{k_s S C_S (1 - X_{CaO}) \sqrt{1 - \psi \ln(1 - X_{CaO})}}{(1 - \varepsilon)} \tag{5}$$

which, when integrated, yields an explicit expression for the kinetic regime:

$$\frac{1}{\psi}\left[\sqrt{1 - \psi \ln(1 - X_{CaO})} - 1\right] = \frac{k_s S C_s t}{2(1 - \varepsilon)} \tag{6}$$

At the other limit, under diffusion through the product layer regime:

$$\frac{\beta Z}{\psi}\left(\sqrt{1-\psi\ln\left(1-X_{CaO}\right)}-1\right)>>1 \tag{7}$$

which allows the equation (2) to be integrated to:

$$\frac{1}{\psi}\left[\sqrt{1-\psi\ln\left(1-X_{CaO}\right)}-1\right]=\frac{S}{\left(1-\varepsilon\right)}\sqrt{\frac{D_P M_{CaO} C_S t}{2\rho_{CaO} Z}} \tag{8}$$

The reaction rate parameters, k_s and D_p, can be obtained by fitting equations (6) and (8) to the experimental data for each regime.

The structural parameters at different cycle numbers were calculated following a method similar to that presented in previous works [54, 56]. This methodology allows the structural parameters of cycled sorbents to be estimated as a function of those corresponding to the fresh calcined limestone and the maximum CO_2 conversion after cycling. These values can then be used to calculate the specific surface area (S_N) and the length of the porous system (L_N) associated with every mixture of particles by means of the following equations:

$$S_N = S_0\ X_N \tag{9}$$

$$L_N = L_0\ X_N \frac{rp_0}{rp_N} \tag{10}$$

The maximum carrying capacity of CO_2 (X_N) can be calculated using the following equation proposed by Grasa et al. [60]

$$X_N = \left(\frac{1}{\frac{1}{\left(1-X_r\right)}+kN}+X_r\right) \tag{11}$$

if the deactivation constant (k) and the residual conversion (x_r) for the limestones are known. Moreover, assuming that the sulfation is homogeneous, it is possible to calculate the product layer thickness from the conversion to $CaSO_4$ using the following expression [53]:

$$\Delta = \frac{2Z(1-\varepsilon)}{\psi S}\left(\sqrt{1-\psi \ln(1-X_{CaO})}-1\right) \quad (12)$$

Equations (6)-(12) will be applied to fit the experimental results following the methodology of section 2.

4. Results and Discussion

The effect of the different variables on the sulphation rates in the CaL reactors have been studied previously [19, 56, 61, 62], including an investigation of the sulphation of the purges from a pilot [19], with the samples being taken from the calciner of the CaL. In these studies it was concluded that the number of calcination carbonation cycles is a variable of special interest. In the present study the experimental work has been broadened to include more limestones and ranges of variables, while the number of calcination carbonation cycles has been strictly controlled in the TG, since it affects the sulphation pattern (surface area, diameter of the pores), in contrast with the previous studies [19, 62]. In the following paragraphs the effect of the main variables (i.e. the SO_2 concentration, the number of calcination carbonation cycles, the reaction temperature, the average particle size, and the presence of other gases such as CO_2 or steam) is described.

The concentration of SO_2 varies depending on the reactors of the CaL system. For example, the SO_2 concentration of the flue gas fed to the carbonator will depend on the sulphur content of the coal being burned in the CFBC as well as on the efficiency of the SO_2 removal process. On the other hand, the maximum SO_2 concentration in the oxy

CFB calciner depends on the composition of the coal burned to achieve the high calcination temperatures. A typical range of inlet concentrations of SO_2 in the entire CaL system can change by about one order of magnitude between 500-3000 ppmv. In the literature [33, 34] a variety of reaction orders generally in the range 0.6-1 have been reported depending on the experimental parameters, although there is relatively general consensus about an apparent first order reaction with respect to the SO_2 reactant. Figure 5a is an example of sulfation experiments carried out with highly cycled materials (N=50) to investigate the effect of the SO_2 concentration at the calciner conditions. As can be seen, as the SO_2 concentration in the bulk gas increases from 500 to 3000 ppmv, there is a proportional effect on the initial slope of sulphation as well as certain impact on the final conversion of CaO to $CaSO_4$. The effect of the SO_2 concentration on the initial reaction rate for the limestones studied at the relevant conditions of all reactors is the CaL is shown in Figure 5b. As it is shown there is an apparent reaction order of 1 at CaL conditions for cycled sorbents.

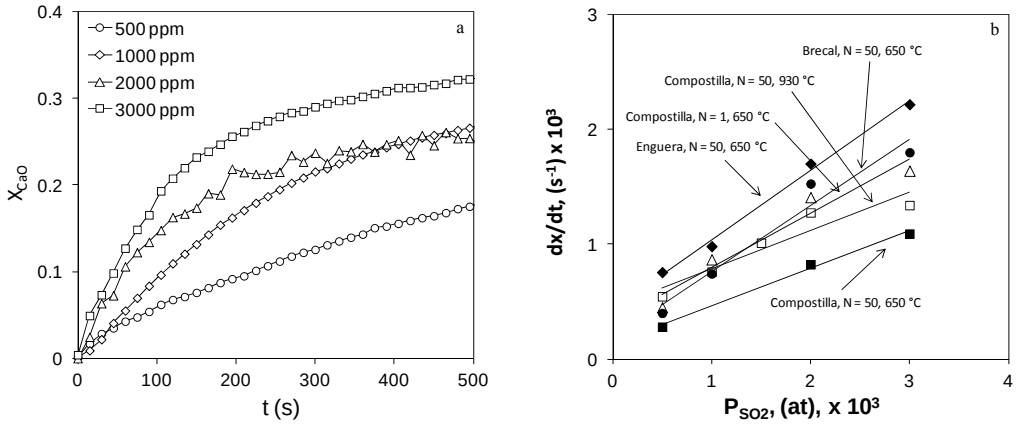

Figure 5. Effect of SO_2 concentration on sulfation of cycled CaO particles. a) conversion curves of Enguera (dp=63-100 μm, 930 °C, N=50) (b) effect of SO_2 concentration on the initial reaction rates for different limes, at two stages of sintering (N = 1,50) and two temperatures (650, 930 °C)

As discussed previously, the number of calcination carbonation cycles, N, has a strong influence on the pore structure of the CaO particles and hence on the sulphation pattern.

It is therefore very important to understand and to be able to quantify the impact of N on the kinetics of the sulphation reactions. The results of experiments conducted for this purpose are represented in Figure 6, which shows the sulphation curves obtained for Enguera lime, cut to a size of 63-100 μm, sulphated under two different sulphation atmospheres. The experiments were carried out with 500 ppm SO_2 in air at 650 ºC for CFB carbonator conditions and 500 ppm SO_2 and 10% vol. CO_2 at 850 ºC for the CFBC conditions.

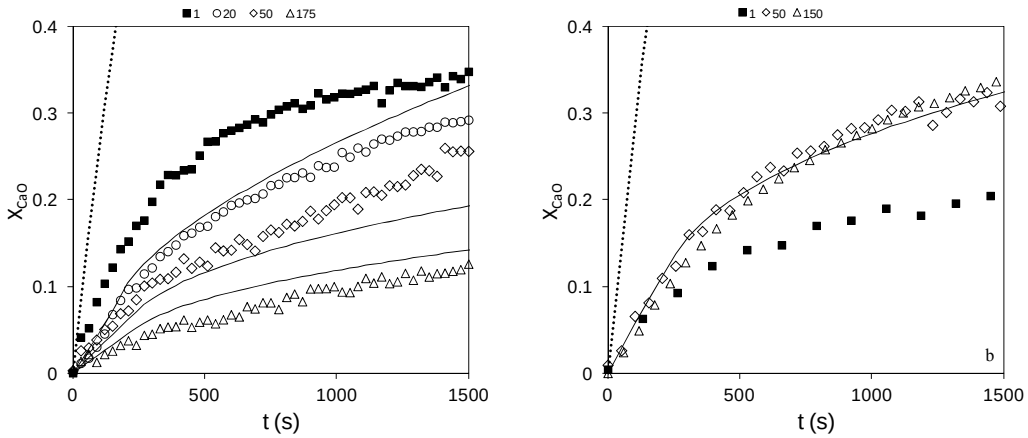

Figure 6. Comparison of the experimental X_{CaO} values of Enguera lime with different numbers of calcination carbonation cycles under the conditions of a CFB carbonator (a) and a CFBC (b). The solid lines correspond to the predictions of the model.

In the carbonator conditions (Figure 6a) it can be seen that as the number of calcination carbonation cycles increases, the sulphation rates and the final conversion of the CaO to $CaSO_4$ at the end of the sulphation test decrease. Maximum sulphation capacity is achieved after one calcination with a X_{CaO} at approximately 0.34 which is very close to the maximum possible sulphation conversion for this sorbent, 0.39. This effect could be due to the reaction surface reduction associated with the increase in the number of calcination carbonation cycles. However, when the reaction temperature increases to 850 ºC, Figure 6b, the trend is quite the opposite despite the reduction in surface area. This is consistent with the pore blockage mechanism as the sulfation conversion after

only one calcination is only 0.17 compared with maximum sulfation conversion. As the pore structure opens up due to the effect of the number of cycles, the inner surface becomes accessible for the reaction to occur and the sulphation conversion increases. Another example of the effect of the number of calcination carbonation cycles on the sulphation curves is shown in Figure 7 for Brecal limestone under the conditions of the CFB carbonator (Figure 7a) and the oxy CFB calciner (Figure 7b). The sulphation in the oxy CFB calciner conditions takes place at 500 ppm SO_2, 70% vol. CO_2 in air at 930 ºC. Under the CFB carbonator conditions (Figure 7a) the initial reaction rate as well as the final sulphation conversion is almost the same after one cycle and after 50 cycles, despite the fact that the surface area has been reduced by around six times after this high number of cycles. This suggests that there is an unreacted core sulphation pattern for the fresh calcined sorbent. As in the previous example, when the reaction temperature increases (CFB calciner conditions), Figure 7b, the sulphation conversion increases when the number of calcination carbonation cycles increases because the pattern tends to become more homogeneous. However, when the cycle number increases to a number as high as 150 cycles, the reduction in surface area predominates over the opening up of the structure, and as a consequence the sulphation conversion is lower than that achieved after 50 cycles.

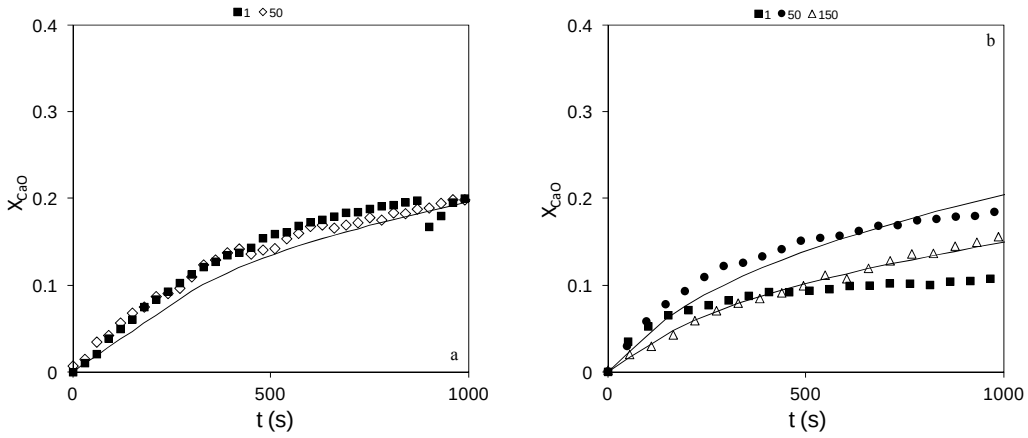

Figure 7. Comparison of X_{CaO} experimental values of Brecal lime with different numbers of calcination carbonation cycles in the conditions of a CFB carbonator (a) and a CFB calciner (b). The solid lines correspond to the predictions of the model.

To summarize, the increase in temperature tends to favour the unreacted core type due to an increase in the internal pore diffusion resistance to the reactant SO_2. By contrast, the carbonation/calcination number tends to favour the homogeneous pattern due to the sintering of the surface that promotes opened-structures.

The RPM was applied to the experimental data yielding the rate constants presented in Table 3. However, cycle 1 was not used for this calculation as this is not typical in a CaL system. The kinetic constants (k_s) were obtained by fitting equation (6) to the experimental X_{CaO} vs time data, in the fast stage of the reaction, whereas the diffusional coefficients through the product layer (D_p) were obtained by fitting equation (8) to the slow regime of the sulphation curves.

Table 3. Kinetic and diffusional constants for the three limestones tested.

	T (°C)	ks (m^4/mol s)	Dp (m^2/s)	EaK (kJ/mol)	k_0 (m^4/mol s)	EaD (kJ/mol)*/**	Dp_0 (m^2/s)*/**
Compostilla	650	4.48E-09	3.53E-12	26.2	1.36E-07	120/53.96	2.18E-5/1.34E-9
	850	8.23E-09	4.14E-12				
	930	9.90E-09	6.08E-12				
Enguera	650	5.75E-09	4.03E-12	21.9	1.01E-07	120/110.7	2.49E-5/1.1E-6
	850	1.03E-08	7.82E-12				
	930	1.08E-08	1.72E-11				
Brecal	650	3.76E-09	1.51E-12	24.9	9.18E-08	120/150.9	9.34E-6/2.97E-5
	850	5.15E-09	2.84E-12				
	930	8.96E-09	8.32E-12				

*/** Below/Above Tammann temperature

For the diffusion through the product layer regime, we applied the Arrhenius equation above 850 ºC but below 850 ºC separately because a slight variation in the E_{aD} fitted under these conditions was detected. This effect has been reported elsewhere in relation with the carbonation reaction of lime [57]. The explanation given in that case was that

above the Tammann temperature (861 ºC [63]), there is a change in the properties of the solid $CaSO_4$ formed, which affects the diffusivity of SO_2 through the product layer, and therefore the E_{aD}. The critical point of regime change is characterized by an experimental X_{CaO}. Consequently, this value was employed in equation (12) to estimate the product layer thicknesses of the regime change, (see Table 4). Although the product layer thicknesses vary in a narrow range at 650 ºC for the three sorbents (i.e. 29.1 nm to 34.3 nm), the range of the estimated thicknesses increases at the other reaction temperatures without a clear tendency. This is due to the difficult in the determination of the critical point of regime change. The change from the fast stage to the diffusional regime control stage is softened as temperature increases and the critical point determined is less accurate.

Table 4. Estimated thicknesses corresponding to the regime changes.

	650 (°C)	850 (°C)	930 (°C)
Compostilla	34.3 nm	13.4 nm	35.4 nm
Enguera	29.3 nm	42.1 nm	20.3 nm
Brecal	29.1 nm	32.2 nm	17.5 nm

As can be seen from Figures 6 and 7, the RPM predicts reasonably well all of the sulphation curves under all the CaL conditions when the cycle number is higher than 20. As might be expected, for cycle 1, the RPM overpredicts the experimental results due to the sulphation pattern and the limitation of our model proposal.

The effect of the particle size is directly related to the sulphation pattern. If the particle size increases, the pore diffusion resistance also increases and consequently unreacted core sulphation patterns are more likely to occur. However, as the number of carbonation calcination cycles changes the pore structure, two samples from Enguera limestone after 20 and 50 cycles were selected to perform the corresponding sulphation tests under two extreme conditions. In addition, the experimental results obtained for

Compostilla after a single calcination in the conditions of an oxy CFB calciner are shown for comparison purposes. After 20 calcination carbonation cycles the sulphation pattern of Enguera was homogeneous for particle sizes below 100 μm sulphated under the conditions of a CFB carbonator, as is shown in Figure 8a. Moreover, both sulphation curves for the two lower cuts are almost identical. However, when the particle size increases to 400-600 μm the sulphation rate clearly decreases, indicating an unreacted core type sulphation pattern for this size. As expected, as the reaction temperature increases, this effect for the sulfation pattern to become non-homogeneous becomes more evident, as in the case of the sulphation reaction under oxy CFB calciner conditions (Figure 8b). The model predicts reasonably well the experimental results corresponding to the three smaller particle sizes, where the pattern is homogeneous. Figure 8c shows an unreacted core pattern, as can be seen from the different X_{CaO} vs time curves obtained for the three different particle sizes of Compostilla lime. This result was to be expected, since the higher particle sizes give rise to a maximum X_{CaO} that is lower than that indicated by its porosity: a value of 0.34 should have been obtained in the absence of pore diffusion resistances.

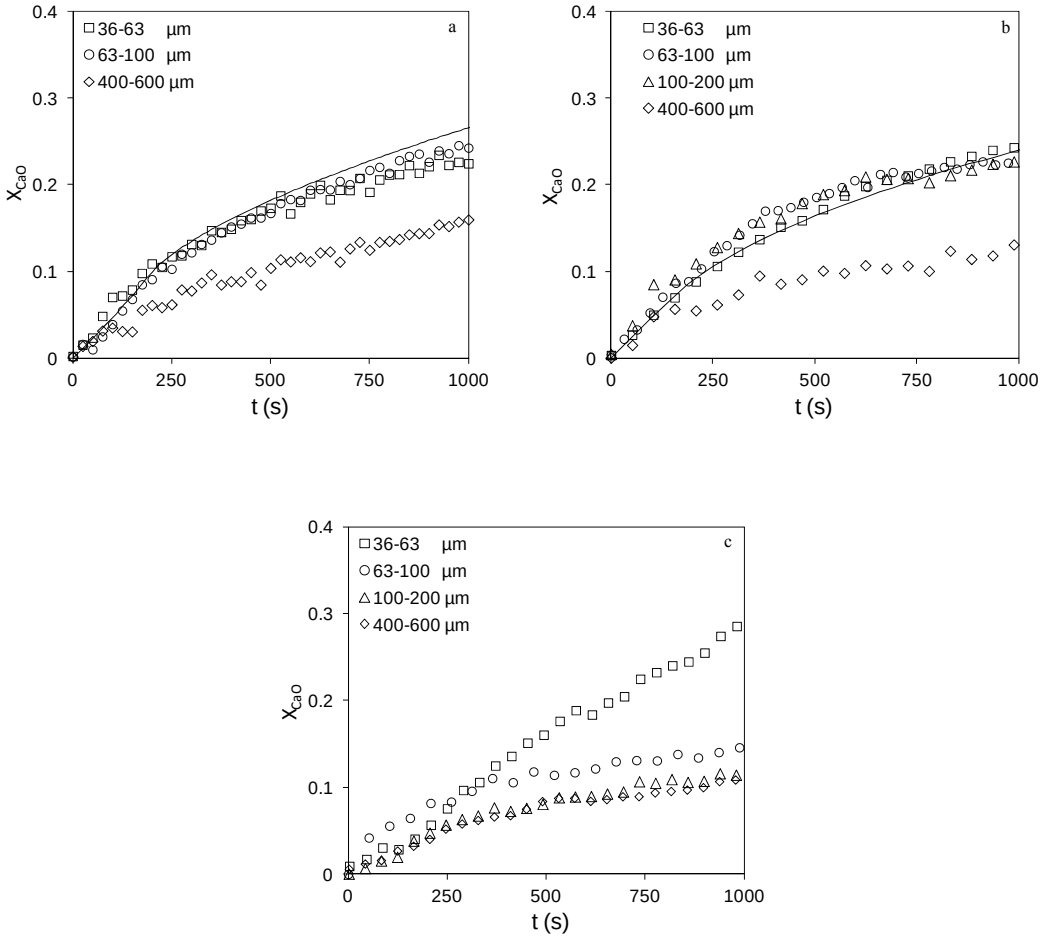

Figure 8. Comparison of the experimental X_{CaO} values of cycled Enguera lime for different particle sizes in the conditions of a CFB carbonator (a) and of a CFB calciner (b). Also the effect of the particle size on the sulphation of Compostilla lime after a single calcination is shown in the conditions of an oxy CFB calciner (c). The solid lines correspond to the predictions of the model.

The effect on the sulphation rates of the CO_2 and H_2O contents in the gas feed was also taken into consideration when there is no competition between carbonation and sulfation reactions. Under CFBC conditions, a typical CO_2 concentration of around 10% vol. was used whereas a CO_2 concentration of 70% vol. under the oxy CFB calciner was selected. CO_2 is a very effective sintering agent [64], so it might affect the internal pore

structure available for sulphation, depending on the time of exposure and the temperature. However, as the sorbent in a CaL will have undergone several cycles of calcination carbonation, the effect of further sintering will be negligible. To test the effect of the CO_2 on the sulphation X_{CaO} vs time curves, two cycled (N = 50) limes were selected and sulphated in CFBC and oxy CFB calciner conditions, with 10% vol. and 70% vol. CO_2 respectively, and 500 ppm SO_2 in air, and compared to the corresponding curves with 0% CO_2. The particle size was 63-100 μm, (see Figure 9). No relevant effects of the CO_2 concentration on the initial sulphation rates of the cycled sorbent can be observed indicating that CO_2 does not affect the sulphation of the cycled lime.

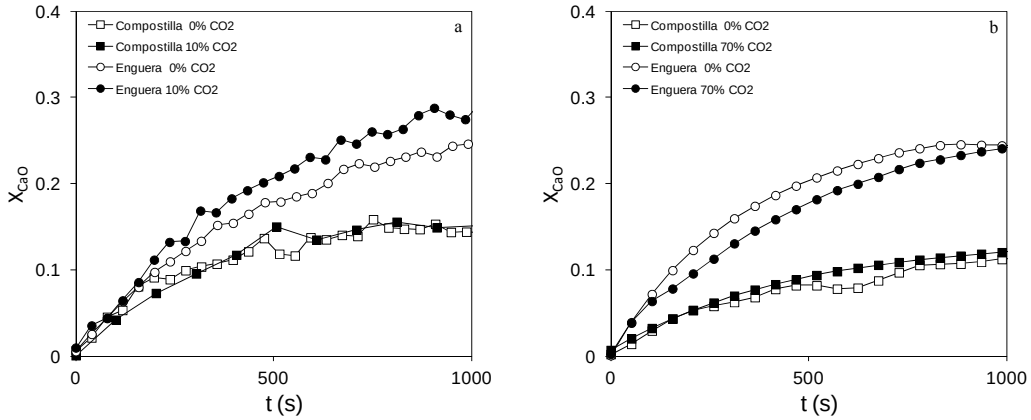

Figure 9. Effect of the CO_2 concentration on the X_{CaO} vs time curves for Enguera and Compostilla limes after 50 cycles of calcination carbonation in the conditions of (a) a CFBC and (b) a CFB calciner.

The experimental data presented until now on the sulphation of CaO were obtained without considering steam. However, steam is a common component of the gas streams produced in power generation. Recently some works [65, 66] have been published that take into account the influence of steam on the sulphation of CaO. They found an enhancement of the sulphur carrying capacities of the limes tested because of an improvement in the rates of diffusion through the product layer. Nevertheless, no appreciable effects were observed on the initial fast step of sulphation. This improvement in the sulphation of CaO is often attributed to a change in the mechanism

of reaction or to a reduction in the resistance to diffusion through the product layer. In this work, the effect of steam was tested using two limestones, Enguera and Compostilla. The CFBC conditions (Figure 10a) were simulated using a mixed gas consisting of 10% vol. CO_2, 500 ppm SO_2, 15 and 30% vol. H_2O in air at 850 ºC. Under oxy CFB calciner conditions (Figure 10b) two reaction mixtures were used: 49% vol. CO_2, 15% vol. H_2O, 500 ppm SO_2 in air, and 36% vol. CO_2, 30% vol. H_2O, 500 ppm SO_2 in air at 930 ºC. The particle size was 63-100 μm and the sulphation tests were performed after 50 calcination carbonation cycles. From the Figure 10a it can be seen that the concentration of steam did not have any effect on the sulphation rates of any of the sorbents. The slopes are essentially the same with and without steam. A slight effect could be noticed for the highest steam concentration used (30%) and Enguera lime at the end of the diffusional regime. The effect is clearer under the oxy CFB calciner conditions. During the first step of reaction where the kinetic controlled regime was predominant (Figure 10b), the steam content had no effect on sulphation conversion during the fast stage, which is consistent with the data reported by other authors [65, 66]. However, the maximum X_{CaO} achieved increased with the steam content. It must be concluded therefore that steam enhances the mechanism of diffusion through the product layer of $CaSO_4$. The X_{CaO} value at which the sulphation rate starts to increase due to the steam is well above 0.1 which is considered as the maximum for CaL systems. Thus in these systems the effect of steam will be negligible.

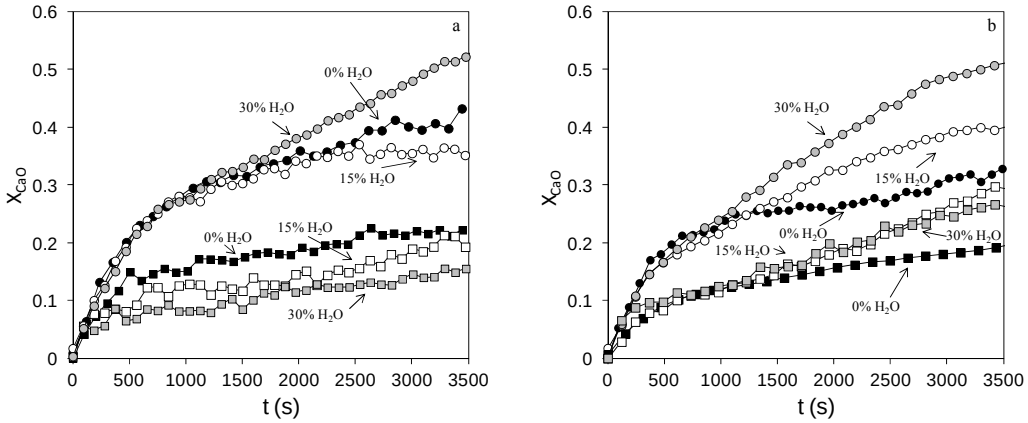

Figure 10. Effect of the H_2O concentration on the X_{CaO} vs time curves for Enguera (○) and Compostilla (□) limes after 50 cycles of calcination carbonation under the conditions of a CFBC (a) and a CFB calciner (b).

5. Conclusions

The reaction order with respect to SO_2 of the sulphation reaction of CaO is always 1 regardless of the reactor conditions in a CaL system. The number of calcination carbonation cycles changes the sulphation pattern becoming more homogeneous as increases. The reaction temperature increase has the opposite effect as the sulphation pattern tends to be unreacted core type due to an increase in diffusional resistance in the pores. The increase in the particle size leads to non-homogeneous sulphation patterns since the length of the pores increases, as does pore diffusional resistance. Nevertheless, for particle sizes below 200 μm and highly cycled sorbents a homogeneous sulphation pattern can be expected at any temperature up to 930 ºC. Dependence on the CO_2 concentration is negligible considering the low conversions to $CaSO_4$ achieved and the high number of cycles to which the sorbent has been subjected. The presence of steam improves the sulphation rates in the slow regime of reaction presumably due to an enhancement of the diffusion through the product layer. The Random Pore Model was

found to be valid for predicting the experimental sulphation rates and capacities of a sorbent sulphated according to a homogeneous pattern.

6. Acknowledgements

The research presented in this work has received partial funding from the European Community Research Fund for Coal and Steel (CaO2 project: RFC-PR-13006). Authors also acknowledge to Prof. J.C. Abanades for his contribution to this article. J.M.C. also acknowledges a Ph.D. fellowship grant awarded by FICYT.

7. Notation

a,b	stoichiometric coefficients for the sulphation reaction
C_S	concentration of SO_2, kmol/m^3
D_P	effective product layer diffusivity, m^2/s
D_{P0}	diffusional pre-exponential factor, m^2/s
d_{pm}	mean pore diameter, nm
E_{ak}	activation energy for the kinetic regime, kJ/mol
E_{aD}	activation energy for the diffusion through the product layer regime, kJ/mol
Δ	product layer thickness, nm
k	sorbent deactivation constant
k_S	rate constant for surface reaction, m^4/mol s
k_{S0}	kinetic pre-exponential factor, m^4/mol s
L	total length of the pore system, m/m^3
M	molecular weight, kg/kmol
N	number of calcination/carbonation cycles
r_{pN}	radius of the pore after N cycles, m
S	reaction surface per unit of volume, m^2/m^3
t	reaction time, s
V_M	molar volume, m^3/kmol
X_N	Maximum CaO molar conversion to $CaCO_3$
X_{CaO}	CaO molar conversion to $CaSO_4$
X^*_{CaO}	Maximum CaO molar conversion to $CaSO_4$
Z	volume fraction ratio before and after reaction
	Greek letters
β	Modified Biot modulus
ε	porosity
ρ	density, kg/m^3
ψ	Internal structure parameter

8. References

[1] IPCC, Special report on carbon dioxide capture and storage, Cambridge University Press, 2005.

[2] T. Shimizu, T. Hirama, H. Hosoda, K. Kitano, M. Inagaki, K. Tejima, A Twin Fluid-Bed Reactor for Removal of CO_2 from Combustion Processes, Chem. Eng. Res. Des., 77 (1999) 62-68.

[3] J.C. Abanades, E.S. Rubin, E.J. Anthony, Sorbent Cost and Performance in CO2 Capture Systems, Ind. Eng. Chem. Res., 43 (2004) 3462-3466.

[4] L.M. Romeo, J.C. Abanades, J.M. Escosa, J. Paño, A. Giménez, A. Sánchez-Biezma, J.C. Ballesteros, Oxyfuel carbonation/calcination cycle for low cost CO2 capture in existing power plants, Energy Conversion and Management, 49 (2008) 2809-2814.

[5] J. Blamey, E.J. Anthony, J. Wang, P.S. Fennell, The calcium looping cycle for large-scale CO2 capture, Prog. Energy Combust. Sci., 36 (2010) 260-279.

[6] I. Martínez, R. Murillo, G. Grasa, J. Carlos Abanades, Integration of a Ca looping system for CO2 capture in existing power plants, AIChE J., 57 (2011) 2599-2607.

[7] Fluidized bed technologies for near-zero emission combustion and gasification, Woodhead Publishing Limited., Cambridge, 2013.

[8] A. Sánchez-Biezma, J.C. Ballesteros, L. Diaz, E. de Zárraga, F.J. Álvarez, J. López, B. Arias, G. Grasa, J.C. Abanades, Postcombustion CO2 capture with CaO. Status of the technology and next steps towards large scale demonstration, Energy Procedia, 4 (2011) 852-859.

[9] B. Arias, M.E. Diego, J.C. Abanades, M. Lorenzo, L. Diaz, D. Martínez, J. Alvarez, A. Sánchez-Biezma, Demonstration of steady state CO2 capture in a 1.7 MWth calcium looping pilot, Int. J. Greenhouse Gas Control, 18 (2013) 237-245.

[10] J. Ströhle, M. Junk, J. Kremer, A. Galloy, B. Epple, Carbonate looping experiments in a 1 MWth pilot plant and model validation, Fuel, 127 (2014) 13-22.

[11] M. Alonso, M.E. Diego, J.C. Abanades, C. Perez, J. Chamberlain, In situ CO_2 capture with CaO in a 300 kW fluidized bed biomass combustor, in: 7th Trondheim CCS Conference, Trondheim, 2013.

[12] C. Hawthorne, H. Dieter, A. Bidwe, A. Schuster, G. Scheffknecht, S. Unterberger, M. Käß, CO2 capture with CaO in a 200 kWth dual fluidized bed pilot plant, Energy Procedia, 4 (2011) 441-448.

[13] M.H. Chang, C.M. Huang, W.H. Liu, W.C. Chen, J.Y. Cheng, W. Chen, T.W. Wen, S. Ouyang, C.H. Shen, H.W. Hsu, Design and Experimental Investigation of Calcium Looping Process for 3-kWth and 1.9-MWth Facilities, Chem. Eng. Technol., 36 (2013) 1525-1532.

[14] D.Y. Lu, R.W. Hughes, E.J. Anthony, Ca-based sorbent looping combustion for CO2 capture in pilot-scale dual fluidized beds, Fuel Process. Technol., 89 (2008) 1386-1395.

[15] J.C. Abanades, M. Alonso, N. Rodríguez, B. González, G. Grasa, R. Murillo, Capturing CO2 from combustion flue gases with a carbonation calcination loop. Experimental results and process development, Energy Procedia, 1 (2009) 1147-1154.

[16] A. Charitos, N. Rodríguez, C. Hawthorne, M.n. Alonso, M. Zieba, B. Arias, G. Kopanakis, G.n. Scheffknecht, J.C. Abanades, Experimental Validation of the Calcium Looping CO2 Capture Process with Two Circulating Fluidized Bed Carbonator Reactors, Ind. Eng. Chem. Res., 50 (2011) 9685-9695.

[17] V. Manovic, E.J. Anthony, D. Loncarevic, SO2 Retention by CaO-Based Sorbent Spent in CO2 Looping Cycles, Ind. Eng. Chem. Res., 48 (2009) 6627-6632.

[18] Y. Li, H. Liu, S. Wu, R. Sun, C. Lu, Sulfation behavior of CaO from long-term carbonation/calcination cycles for CO2 capture at FBC temperatures, J. Therm. Anal. Calorim., 111 (2013) 1335-1343.

[19] J.M. Cordero, M. Alonso, B. Arias, J.C. Abanades, Sulfation Performance of CaO Purges Derived from Calcium Looping CO2 Capture Systems, Energy & Fuels, 28 (2014) 1325-1330.

[20] M.E. Diego, B. Arias, M. Alonso, J.C. Abanades, The impact of calcium sulfate and inert solids accumulation in post-combustion calcium looping systems, Fuel, 109 (2013) 184-190.

[21] P. Sun, J.R. Grace, C.J. Lim, E.J. Anthony, Removal of CO2 by Calcium-Based Sorbents in the Presence of SO2, Energy Fuels, 21 (2006) 163-170.

[22] G.S. Grasa, M. Alonso, J.C. Abanades, Sulfation of CaO Particles in a Carbonation/Calcination Loop to Capture CO2, Ind. Eng. Chem. Res., 47 (2008) 1630-1635.

[23] V. Manovic, E.J. Anthony, Competition of Sulphation and Carbonation Reactions during Looping Cycles for CO2 Capture by CaO-Based Sorbents†, J. Phys. Chem. A, 114 (2010) 3997-4002.

[24] B. Arias, G.S. Grasa, M. Alonso, J.C. Abanades, Post-combustion calcium looping process with a highly stable sorbent activity by recarbonation, Energy Environ. Sci., 5 (2012) 7353-7359.

[25] V. Manovic, E.J. Anthony, Carbonation of CaO-Based Sorbents Enhanced by Steam Addition, Ind. Eng. Chem. Res., 49 (2010) 9105-9110.

[26] E.J. Anthony, D.L. Granatstein, Sulfation phenomena in fluidized bed combustion systems, Prog. Energy Comb. Sci., 27 (2001) 215-236.

[27] R.H. Borgwardt, Kinetics of the reaction of sulfur dioxide with calcined limestone, Environ. Sci. Technol., 4 (1970) 59-63.

[28] R.H. Borgwardt, R.D. Harvey, Properties of carbonate rocks related to sulfur dioxide reactivity, Environ. Sci. Technol., 6 (1972) 350-360.

[29] R.L. Pigford, G. Sliger, Rate of Diffusion-Controlled Reaction Between a Gas and a Porous Solid Sphere - Reaction of SO2 with CaCO3, Industrial & Engineering Chemistry Process Design and Development, 12 (1973) 85-91.

[30] M. Hartman, R.W. Coughlin, Reaction of Sulfur Dioxide with Limestone and the Influence of Pore Structure, Industrial & Engineering Chemistry Process Design and Development, 13 (1974) 248-253.

[31] M. Hartman, R.W. Coughlin, Reaction of sulfur dioxide with limestone and the grain model, AIChE J., 22 (1976) 490-498.

[32] M. Hartman, O. Trnka, Influence of temperature on the reactivity of limestone particles with sulfur dioxide, Chem. Eng. Sci., 35 (1980) 1189-1194.

[33] S.K. Bhatia, D.D. Perlmutter, The effect of pore structure on fluid-solid reactions: Application to the SO2-lime reaction, AIChE J., 27 (1981) 226-234.

[34] R.H. Borgwardt, K.R. Bruce, Effect of specific surface area on the reactivity of CaO with SO2, AIChE J., 32 (1986) 239-246.

[35] J.S. Dennis, A.N. Hayhurst, Mechanism of the sulphation of calcined limestone particles in combustion gases, Chem. Eng. Sci., 45 (1990) 1175-1187.

[36] M. Hartman, O. Trnka, Reactions between calcium oxide and flue gas containing sulfur dioxide at lower temperatures, AIChE J., 39 (1993) 615-624.

[37] J. Adanez, P. Gayan, F. Garcia-Labiano, Comparison of Mechanistic Models for the Sulfation Reaction in a Broad Range of Particle Sizes of Sorbents, Ind. Eng. Chem. Res., 35 (1996) 2190-2197.

[38] J. Adánez, F. García-Labiano, V. Fierro, Modelling for the high-temperature sulphation of calcium-based sorbents with cylindrical and plate-like pore geometries, Chem. Eng. Sci., 55 (2000) 3665-3683.

[39] F. García-Labiano, A. Rufas, L.F. de Diego, M.d.l. Obras-Loscertales, P. Gayán, A. Abad, J. Adánez, Calcium-based sorbents behaviour during sulphation at oxy-fuel fluidised bed combustion conditions, Fuel, 90 (2011) 3100-3108.

[40] D. Alvarez, J.C. Abanades, Pore-Size and Shape Effects on the Recarbonation Performance of Calcium Oxide Submitted to Repeated Calcination/Recarbonation Cycles, Energy Fuels, 19 (2004) 270-278.

[41] K. Laursen, W. Duo, J.R. Grace, J. Lim, Sulfation and reactivation characteristics of nine limestones, Fuel, 79 (2000) 153-163.

[42] J. Szekely, J.W. Evans, H.Y. Sohn, Gas-solid reactions, (1976).

[43] S.V. Sotirchos, H.C. Yu, Overlapping grain models for gas-solid reactions with solid product, Ind. Eng. Chem. Res., 27 (1988) 836-845.

[44] P.A. Ramachandran, J.M. Smith, Effect of sintering and porosity changes on rates of gas—solid reactions, The Chemical Engineering Journal, 14 (1977) 137-146.

[45] C. Georgakis, C.W. Chang, J. Szekely, A changing grain size model for gas--solid reactions, Chem. Eng. Sci., 34 (1979) 1072-1075.

[46] P.V. Ranade, D.P. Harrison, The grain model applied to porous solids with varying structural properties, Chem. Eng. Sci., 34 (1979) 427-432.

[47] K. Dam-Johansen, P.F.B. Hansen, K. Østergaard, High-temperature reaction between sulphur dioxide and limestone—III. A grain-micrograin model and its verification, Chem. Eng. Sci., 46 (1991) 847-853.

[48] J. Szekely, M. Propster, A structural model for gas solid reactions with a moving boundary—VI: The effect of grain size distribution on the conversion of porous solids, Chem. Eng. Sci., 30 (1975) 1049-1055.

[49] E.E. Petersen, Reaction of porous solids, AIChE J., 3 (1957) 443-448.

[50] P.A. Ramachandran, J.M. Smith, A single-pore model for gas-solid noncatalytic reactions, AIChE J., 23 (1977) 353-361.

[51] G.A. Simons, A.R. Garman, A.A. Boni, The Kinetic rate of SO_2 sorption by CaO, AIChE J., 33 (1987) 211-217.

[52] S.K. Bhatia, D.D. Perlmutter, A random pore model for fluid-solid reactions: I. Isothermal, kinetic control, AIChE J., 26 (1980) 379-386.

[53] S.K. Bhatia, D.D. Perlmutter, A random pore model for fluid-solid reactions: II. Diffusion and transport effects, AIChE J., 27 (1981) 247-254.

[54] G. Grasa, R. Murillo, M. Alonso, J.C. Abanades, Application of the random pore model to the carbonation cyclic reaction, AIChE J., 55 (2009) 1246-1255.

[55] H. Ale Ebrahim, Application of Random-Pore Model to SO2 Capture by Lime, Ind. Eng. Chem. Res., 49 (2009) 117-122.

[56] B. Arias, J.M. Cordero, M. Alonso, J.C. Abanades, Sulfation rates of cycled CaO particles in the carbonator of a Ca-looping cycle for postcombustion CO2 capture, AIChE J., 58 (2012) 2262-2269.

[57] S.K. Bhatia, D.D. Perlmutter, Effect of the product layer on the kinetics of the CO2-lime reaction, AIChE J., 29 (1983) 79-86.

[58] M. Alonso, Y.A. Criado, J.C. Abanades, G. Grasa, Undesired effects in the determination of CO2 carrying capacities of CaO during TG testing, Fuel, 127 (2014) 52-61.

[59] H.-J. Ryu, J.R. Grace, C.J. Lim, Simultaneous CO2/SO2 Capture Characteristics of Three Limestones in a Fluidized-Bed Reactor, Energy Fuels, 20 (2006) 1621-1628.

[60] G.S. Grasa, J.C. Abanades, CO2 Capture Capacity of CaO in Long Series of Carbonation/Calcination Cycles, Ind. Eng. Chem. Res., 45 (2006) 8846-8851.

[61] M. Alonso, J.M. Cordero, B. Arias, J.C. Abanades, Sulfation Rates of Particles in Calcium Looping Reactors, Chemical Engineering & Technology, 37 (2014) 15-19.

[62] B. Arias, J.M. Cordero, M. Alonso, M.E. Diego, J.C. Abanades, Investigation of SO2 Capture in a Circulating Fluidized Bed Carbonator of a Ca Looping Cycle, Industrial & Engineering Chemistry Research, 52 (2013) 2700-2706.

[63] A.P. Iribarne, J.V. Iribarne, E.J. Anthony, Reactivity of calcium sulfate from FBC systems, Fuel, 76 (1997) 321-327.

[64] R. H. Borgwardt, Sintering of nascent calcium oxide, Chem. Eng. Sci., 44 (1989) 53-60.

[65] C. Wang, L. Jia, Y. Tan, E.J. Anthony, The effect of water on the sulphation of limestone, Fuel, 89 (2010) 2628-2632.

[66] M.C. Stewart, V. Manovic, E.J. Anthony, A. Macchi, Enhancement of Indirect Sulphation of Limestone by Steam Addition, Environ. Sci. Technol., 44 (2010) 8781-8786.